Experimental study on a novel manual wheelchair

Technology and Disability -1 (2023) 1–11
DOI 10.3233/TAD-220395
IOS Press

Experimental study on a novel manual wheelchair

Andrea Botta*, Paride Cavallone, Luigi Tagliavini and Giuseppe Quaglia
Department of Mechanical and Aerospace Engineering, Politecnico di Torino, Torino, Italy

Received 9 September 2022
Accepted 29 January 2023

Abstract.
BACKGROUND: Traditional manual wheelchair users suffer from upper limbs injuries due to the propulsion gesture.
OBJECTIVE: This paper presents the experimental activity addressed to define the dynamic characteristics of a novel manual wheelchair. The design and realization of the wheelchair aim to reduce injuries of the upper limbs related to conventional wheelchairs. A new index called *Peak Of Force*, *POF*, is defined and applied to the different wheelchair manual propulsion systems.
METHODS: The wheelchair speed and the left and right-hand forces exerted by the user are monitored. The tests have been performed by changing the transmission ratio of the wheelchair and the wheelchair speed.
RESULTS: The indices *MEF* and *FEF* are lower than 100% due to the lateral and radial forces for hand-rim wheelchairs and handbikes. For Handwheelchair.Q these indices are equal to 100%. The mean value of index *POF* for Handwheelchair.Q is 51.75%, while it is about 42.5% for the hand-rim wheelchair, and 57.6% for the handbike.
CONCLUSIONS: The user forces for Handwheelchair.Q depend on the wheelchair speed and the pulley radius. The larger pulley radius reduces the average and the maximum force. A variable transmission ratio can be implemented on the proposed wheelchair.

Keywords: Manual wheelchair, Handwheelchair.Q, spinal cord injury

1. Introduction

Wheelchair users often present injuries and pain of the upper extremity joints due to the overuse of the upper limbs [1]. In fact, many daily activities as wheelchair propulsion and transfers strongly overload the wrist, the elbow, and the shoulder joints [2]. The pain of the upper limbs interferes significantly with their personal life with repercussions on a psychological level [3,4]. There are different possibilities to reduce injuries of the upper limbs, such as optimizing the handrim wheelchair propulsion [5,6], optimising or using devices for the transfers [7,8], and using an alternative system of propulsion, manual or electric, in order to avoid the same repetitive mechanical loading [9,10]. For wheelchair users, practising physical activity [11,12] is an essential tool for rehabilitation from a physical and psychological point of view [13]. There are different modes of manual propulsion such as handbike [14], lever system [15] as well as handrim. Table 1 summarises the main architectures advantages, drawbacks and principal use.

In this scenario, the research group at the Politecnico di Torino has designed an innovative prototype of a wheelchair named “Handwheelchair.Q” characterised by an alternative propulsion system described in detail in different papers [16–19]. The prototype, shown in Fig. 1, is based on a frame of a standard lightweight wheelchair with an adjustable seat.

Two cables, one per side, to spin the wheels. Each cable is wrapped around a pulley connected to the wheel with a freewheel; then, it goes around a return pulley mounted on a telescopic rod and ends with a handle

*Corresponding author: Andrea Botta, Department of Mechanical and Aerospace Engineering, Politecnico di Torino, Corso Duca degli Abruzzi, 24, 10129 Torino, Italy. E-mail: andrea.botta@polito.it.

ISSN 1055-4181/$35.00

Table 1
Main wheelchair architectures and their advantages, drawbacks and typical usage

Architecture	Pros	Cons	Typical use
Hand-rim	Simple Compact Turn on the spot	Propulsion gesture in a fixed plane Can lead to shoulder joint overuse and pain Not suited for long distances	Every day use Indoor and outdoor
Handbike	Suited for long distances User applies almost constant force Has a transmission system	Propulsion gesture in a fixed plane Not suited for indoor activities Can't turn on the spot It is a dedicated wheelchair	Long distances Sport activities Outdoor

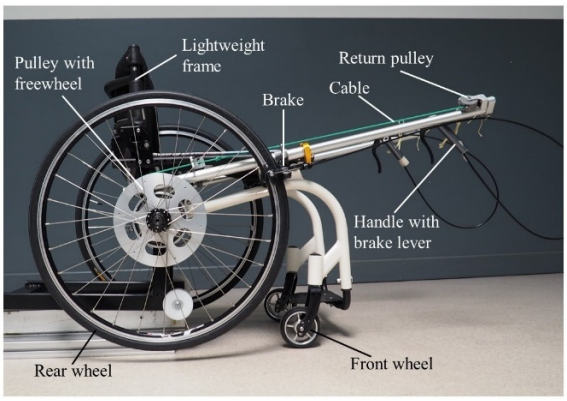

Fig. 1. Prototype of Handwheelchair.Q.

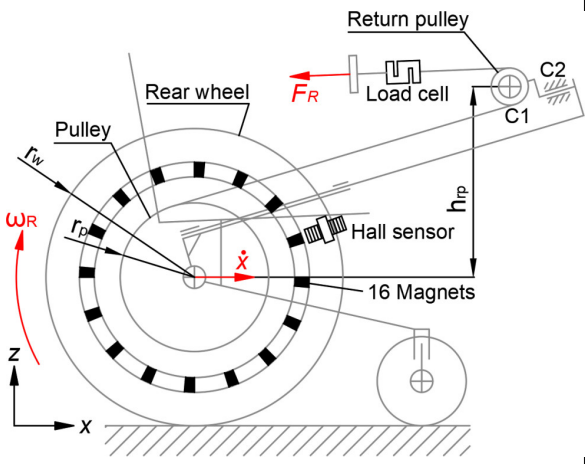

Fig. 2. Handwheelchair.Q scheme and variable definition.

with the brake lever. The return pulley enables the user to drive the wheelchair by pulling the cable using a movement similar to that of rowing. Figure 2 shows how the return pulley is connected to the frame with a joint *C2*. The return pulley has two degrees of freedom, it can rotate around joint *C1* and can pivot around the joint *C2*. This solution has been adopted in order to limit the friction of the cable on the two sides of the pulley, and for having a self-adapting pulling direction imposed by the user. In addition to that, the telescopic rod regulates the return pulley distance and height to accommodate a wide range of users.

Handwheelchair.Q is driven similarly to conventional hand-rim wheelchairs except for the way the user produces the propulsive force. If similar forces are applied by the user on the left and right sides, the wheelchair goes straight. If more force is applied to one side instead, the wheelchair turns to the side where less force is applied. If needed, the user can still use the hand-rims of Handwheelchair.Q to manoeuvre in tight places (the telescopic rods can be retracted), to rotate on the spot, or to go backwards.

The ratio between the rear wheel radius r_w and the pulley radius r_p defines the transmission ratio of Handwheelchair.Q. The pulley radius can be changed in order to optimise the transmission ratio for each user. The aforementioned handrim, lever system, and handbike manual propulsion systems have a common characteristic: the trajectory of the gesture is fixed. This means that the force of the user has three components, but only the tangential component is useful for the transmission of motion. Handwheelchair.Q, instead, uses a cable transmission in which the user force is entirely helpful for the transmission of motion. Multiple studies have investigated the efficiency of common propulsion systems and different indices such as *FEF*, *Fraction Effective Force*, and *MEF*, *Mechanical Effective Force*, to compare different systems of propulsion [20,21]. These indices are described in detail in the discussion paragraph, and they are used to assess the performance of the proposed solution compared to the more typical ones. The aim of this paper is to define the dynamic characteristics of a manual wheelchair with an innovative rowing motion and to determine a new performance index in order to compare different manual wheelchairs.

2. Methods

2.1. Subject

One able-bodied subject (29 years old, 170 cm, 65 kg) not familiar with wheelchair use, participated

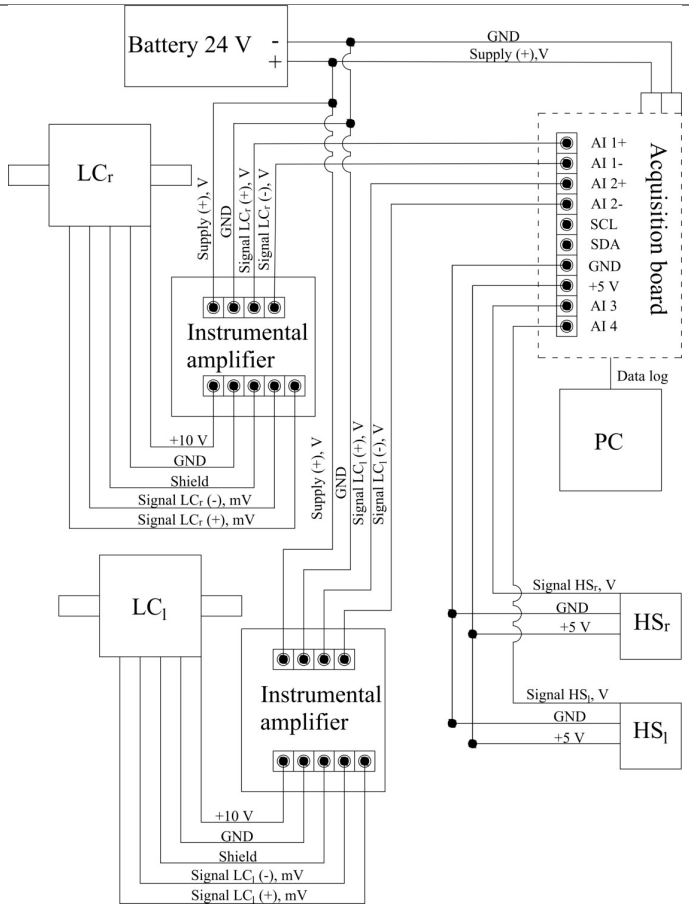

Fig. 3. Circuit diagram of the acquisition system.

in the experiment. This experimental test is a preliminary analysis of the dynamic of an innovative manual wheelchair, hence, in the preliminary test nobody else was involved. The limitation of having just one able-bodied male user is clear, however, each test was repeated several times in order to obtain reliable results. Prior to the trials, the participant provided written informed consent. Ethical approval was granted, and the work was performed in accordance with the Declaration of Helsinki.

2.2. Equipment

Two load cells, (Manufacturer: LCM Systems Ltd, Model DCE, City: Newport, Country: United kingdom) connected the handles with the traction cable to measure the user input forces F_R (right hand) and F_L (left hand), as shown in Fig. 2.

Specification of the load cells:

- Rated load: 500 N,
- Non-Linearity $< \pm\ 0.25\%$ of rated load,
- Non-Repeatability $< 0.1\%$ of rated load.

The angular speeds of the right and left wheels, ω_R and ω_L respectively, were obtained by measuring the frequency of the output signal of a hall sensor (Manufacturer: Honeywell, Model: SS490 MRL, City: Charlotte, Country: North Carolina, USA) mounted on the wheelchair frame that detects the passages of sixteen equidistant magnets positioned on each wheel, Fig. 2.

2.3. Data acquisition

Force and angular speed data were recorded with a National Instrument USB-6341 data acquisition device with 1000 Hz sampling frequency. Such data are collected by the on-board PC and then they are processed offline. The data processing phase mainly involves applying a proper low-pass zero-phase digital filter to the data and to compute all significant quantities that can be derived from the raw data. The circuit diagram of the acquisition system is detailed in Fig. 3.

2.4. Data processing

Once an experimental trial has been completed, the collected data, namely the left and right wheel angular speeds, ω_L and ω_R respectively, and the user exerted forces with the left and right hands, F_L and F_R respectively, are filtered by means of low-pass filters. After that, it is possible to compute some quantities useful to analyse the wheelchair behaviour. From the wheels angular speed, it is possible to compute the wheelchair longitudinal velocity $\dot{x}$ as follows:

$$\dot{x} = \frac{\omega_R + \omega_L}{2} r_w \tag{1}$$

where r_w is the rear wheel radius.

Furthermore, it is convenient to define the whole force exerted by the user F_i during the i-th cycle as:

$$F_i = F_{R,i} + F_{L,i} \tag{2}$$

To uniformly compare the test runs, the mean steady-state force exerted by the user over the measured cycles F is defined as:

$$F = \frac{\sum_6^n F_i}{n-5} \tag{3}$$

where the subscript n is the number of the total cycles of the run and the steady-state phase starts at the 6$^{\text{th}}$ cycle, with $i = 6$.

The rowing gesture is characterised by two distinct phases: an active phase, when the user pulls the cables to propel the wheelchair, and a recovery phase, when the user let the cables go back to their initial position thanks to the retractable cable reel mechanism in the pulleys. Therefore, it is possible to identify a period T_A that corresponds to the duration of an active phase and, conversely, a period T_R corresponding to the recovery phase. In practical terms, T_A is the duration of the active phase measured whenever the user forces are above the threshold value of 5 N (the resolution of the load cells plus a safety range). Conversely, T_R is the time in which the user forces are below the threshold. Hence, the overall rowing gesture period can be defined as $T = T_A + T_R$. $F1$, defined by Eq. (4) is the average force during the complete cycle T, while $F2$, defined by the Eq. (5) is the average force during the active phase, T_A, and F_{max} is the peak of F.

$$F1 = \frac{1}{T} \int_0^T F \, dt \tag{4}$$

$$F2 = \frac{1}{T_A} \int_0^{T_A} F \, dt \tag{5}$$

The input powers PI_i of all the cycles of the steady state phase is:

$$PI_i = F_{R,i} r_p \omega_{R,i} + F_{L,i} r_p \omega_{L,i} \tag{6}$$

where r_p is the pulley radius. Their average over a single run PI is:

$$PI = \frac{\sum_6^n PI_i}{n-5} \tag{7}$$

where the subscript n is the number of the total cycles of the run and the steady-state phase starts at the 6$^{\text{th}}$ cycle, with $i = 6$.

Similarly to the forces, the average user power over a gesture cycle $PI1$ and over the active phase $PI2$ are defined as follows:

$$PI1 = \frac{1}{T} \int_0^T PI \, dt \tag{8}$$

$$PI2 = \frac{1}{T_A} \int_0^{T_A} PI \, dt \tag{9}$$

At last, the user exerted energy during the active phase is:

$$EI = \int_0^{T_A} PI \, dt \tag{10}$$

2.5. Experimental tests

The experimental tests consisted of propelling Handwheelchair.Q from a standing start on a flat hallway covered with a dotted rubber flooring. The user was asked to drive the wheelchair for about 60 m with different intensities (low or high) and different transmission ratios. The low intensity has been defined as the intensity at which the user does not perceive fatigue, comparable to a walk on a flat surface, that corresponds to approximately 1.5 m/s. The high intensity has been defined by increasing the wheelchair speed by 50%, thus it corresponds to a velocity of about 2 m/s. In the tests, the user was able to check the wheelchair speed in real time with a speedometer to verify that he was moving at a speed close to the desired one and to adjust the rhythm of the rowing gesture accordingly. The user was able to maintain an average speed of 1.57 $\pm$ 0.09 m/s during the low intensity tests and an average velocity of 2.33 $\pm$ 0.05 m/s during the high intensity ones.

Four sets of tests were performed, each one composed of five runs (A, B, C, D, and E):

- Test 1: “Low speed” with the radius pulley r_{p1};
- Test 2: “Low speed” with the radius pulley r_{p2};
- Test 3: “High speed” with the radius pulley r_{p1};
- Test 4: “High speed” with the radius pulley r_{p2}.

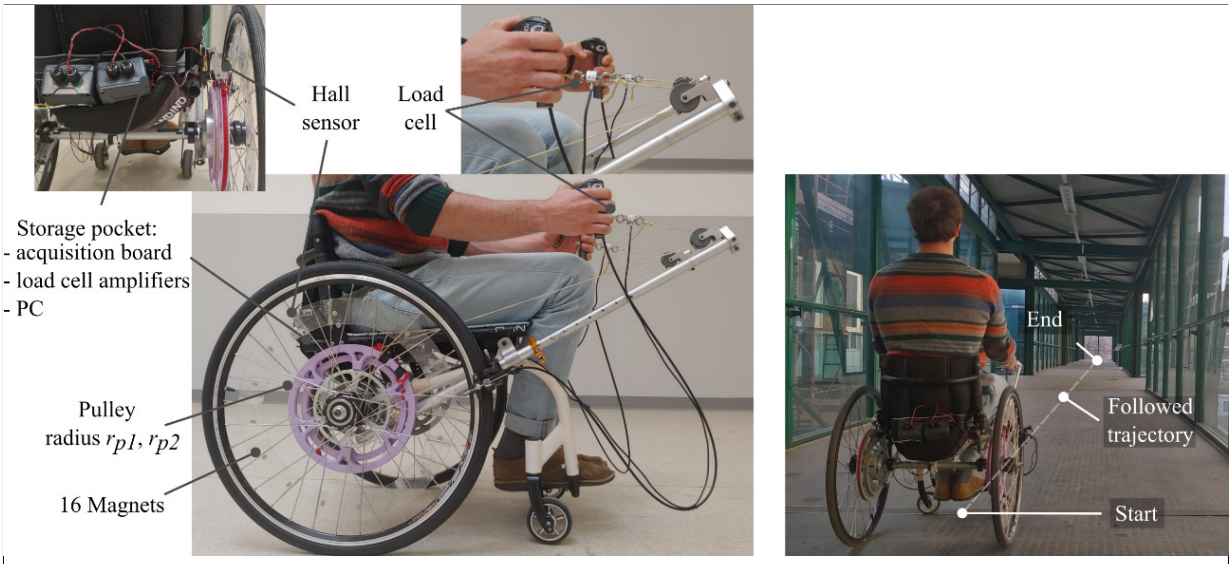

Fig. 4. Handwheelchair.Q experimental setup.

Where the two different pulley radii used were $r_{p1} = 108$ mm and $r_{p2} = 130$ mm and the radius of the rear wheels was $r_w = 292$ mm.

Also, before all tests, the height of the return pulley, h_{rp}, was chosen by the user in order to get a comfortable rowing motion based on his personal feelings and was kept constant. Such position defines the rowing gesture direction since it defines the direction in which the user pulls the cables to propel the wheelchair. Hence the user was able to set the wheelchair return pulley position to match his preferences and size. Figure 4 presents the experimental setup and the test environment.

2.6. Performance indices

Being that the force peaks are dangerous for the upper limb joints [22], it is important to define a new index, called *POF*, *Peak of Force*, in order to evaluate the peaks of force. The higher the index is, the better, in order to reduce the peaks of force. The index *POF* is defined as:

$$POF = \frac{F_u}{F_{max}} \tag{11}$$

where F_u is the mean over the active phase of the useful component of the total force F exerted by the user (left and right hand contributions are added together), i.e., it is the only portion of user exerted force contributing to the wheelchair propulsion. The useful component F_u that produces the wheelchair motion depends on the wheelchair propulsion system. F_{max}, instead, is the peak value of the total force F applied by the user. In other terms, the *POF* index compares the maximum total force and the average useful force exerted by the user with different wheelchair architectures. A *POF* close to 1 means that, in the corresponding propulsion architecture, the average value of the useful force and the peak value of the total force are similar and therefore there are limited peaks of force during the wheelchair operation and the exerted force is almost constant. Conversely, a low *POF* index represents an architecture where the user-exerted force varies considerably and there are significant peaks of force during the wheelchair use.

In a standard wheelchair with a hand rim system of radius r_{hr}, only the portion of exerted force tangential to the hand rim, F_{tan}, contributes to the rotation of the wheels, all the other components are wasted instead. Hence, $F_u = F_{tan}$ in traditional wheelchairs. Similarly, in handbikes, the portion of the user-exerted force that is tangential to the hand crank is the useful force contributing to the motion. In the proposed novel wheelchair, Handwheelchair.Q, the whole force exerted by the user pulling the cable is transmitted to the pulley to produce motion, therefore, in this case, the useful force corresponds to the whole pulling force.

In literature also exists other indices to evaluate wheelchair performance. The indices *MEF* (*mechanical effective force*) and *FEF* (*fraction effective force*), are defined. by Eq. (3) [23] and Eq. (4) [24], respectively. The two indices measure in a slightly different way how much of the user exerted force is used to produce motion. The difference between *MEF* and *FEF* is

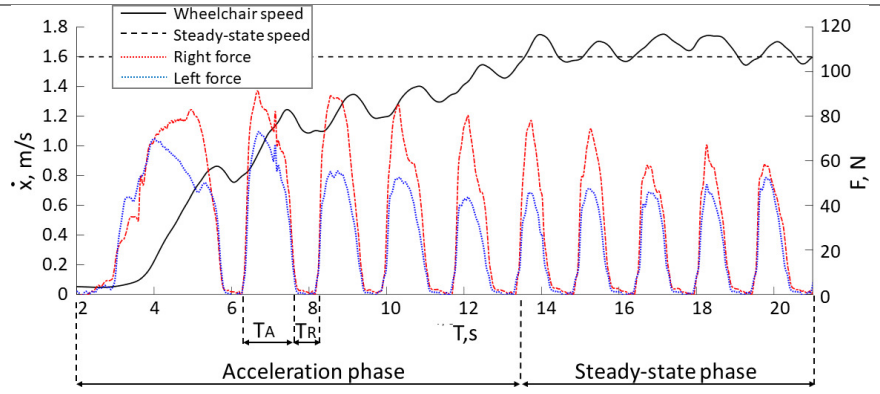

Fig. 5. Wheelchair speed, in black, right force, in red, and left force, in blue, during the test. T_A represents the duration of the active propulsion phase, while T_R is the duration of the recovery phase.

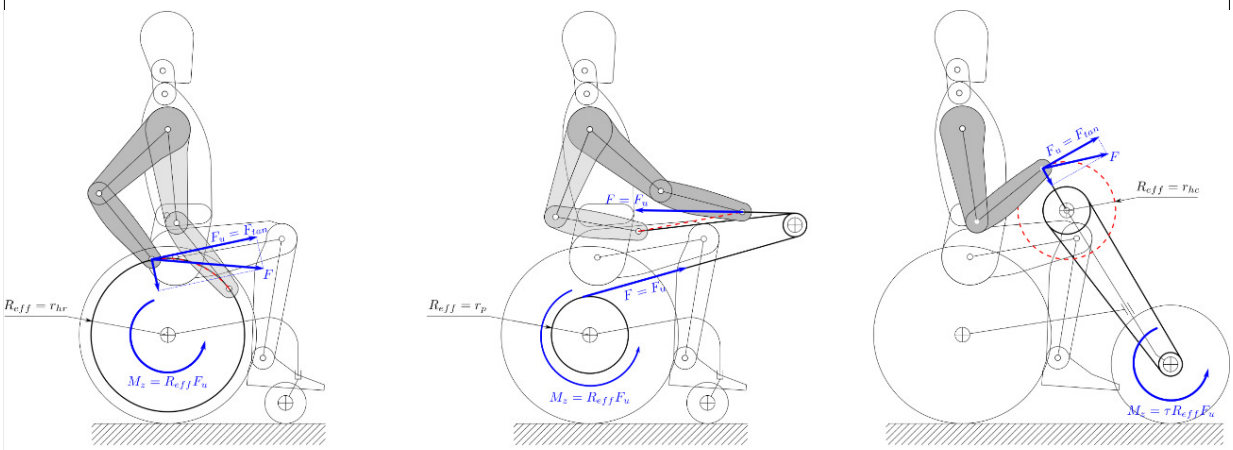

Fig. 6. Diagram showing the useful force F_u for each configuration.

that the *MEF* does not take into account the "gripping moment" [24].

$$F = \sqrt{F_x^2 + F_y^2 + F_z^2} \tag{12}$$

$$M_z = \tau R_{eff} F_u \tag{13}$$

$$MEF = \frac{F_u^2}{F^2} \cdot 100 \tag{14}$$

$$FEF = \frac{M_z}{R_{eff} F} \cdot 100 \tag{15}$$

where F is the whole force exerted by the user, F_u is the useful component of F that contributes to motion, M_z is the torque applied to the wheel, R_{eff} is the lever arm of F_u that produces M_z, and τ is the architecture transmission ratio.

In the case of hand-rim wheelchairs and the proposed one, the transmission ratio τ is 1 since the useful force F_u directly produce a torque on the wheel. In hand-bikes, usually, there is a transmission system between the hand-crank and the wheel. The effective radius R_{eff} in a hand-rim wheelchair is the radius of the hand-rim and the useful force F_u is the tangential component of F to the hand-rim. In the proposed wheelchair, the effective radius R_{eff} is the pulley radius r_p and the useful force is the whole force exerted by the user F. At last, in a hand-crank wheelchair, the effective radius R_{eff} is the hand-crank radius r_{hc} and the useful force is the one tangential to it. Figure 6 depicts a diagram for each configuration.

3. Results

Each test was performed five times, each run is composed of two phases: the acceleration phase and the steady-state phase. During the acceleration phase, the

Table 2

Mean (SD). $F_{i,max}$ in acceleration phase is the maximum force in a specific cycle, $F1$ is the average force in the complete cycle, $F2$ is the average force in the active phase, Fmax is the peak of force F in the steady-state phase, *PI*1 is the input power in the complete cycle, *PI*2 is the input power in the active phase, *TA* is the time of the active phase, *TR* is the time of the recovery phase, *EI* is the input energy and is the average wheelchair speed in the steady-state phase

		Low speed		High speed	
		Test 1	Test 2	Test 3	Test 4
Acceleration phase	$F_{1,max}$	141 (1.9)	146 (12.9)	222 (16.6)	223 (10.8)
	$F_{2,max}$	163 (9.8)	172 (6.1)	255 (8.6)	242 (9.0)
	$F_{3,max}$	155 (12.7)	148 (9.5)	225 (7.0)	221 (15.1)
	$F_{4,max}$	136 (11.3)	134 (5.6)	211 (24.2)	175 (18.3)
	$F_{5,max}$	114 (11.9)	118 (11.2)	180 (24.4)	181 (24.3)
Steady-state phase	$F1$ [N]	37.5 (3.8)	30.3 (5.8)	45.3 (4.7)	40.1 (3.9)
	$F2$ [N]	57.6 (1.8)	51.6 (2.5)	76.4 (4.2)	60.9 (2.7)
	F_{max} [N]	101.4 (4.2)	95.4 (1.7)	147.2 (6.8)	133.2 (6.3)
	*PI*1 [W]	20.9 (3.2)	21.9 (4.4)	38.3 (8.7)	42.1 (2.44)
	*PI*2 [W]	33.7 (1.7)	39.1 (1.8)	67.5 (4.3)	66.9 (0.98)
	T_A [s]	0.99 (0.03)	0.84 (0.04)	0.70 (0.05)	0.60 (0.02)
	T_R [s]	0.53 (0.01)	0.59 (0.06)	0.48 (0.04)	0.43 (0.03)
	EI [J]	33.3 (2.7)	32.8 (3.0)	47.2 (6.3)	40.1 (1.9)
	$\bar{x}$ [m/s]	1.51 (0.04)	1.63 (0.05)	2.29 (0.09)	2.36 (0.09)

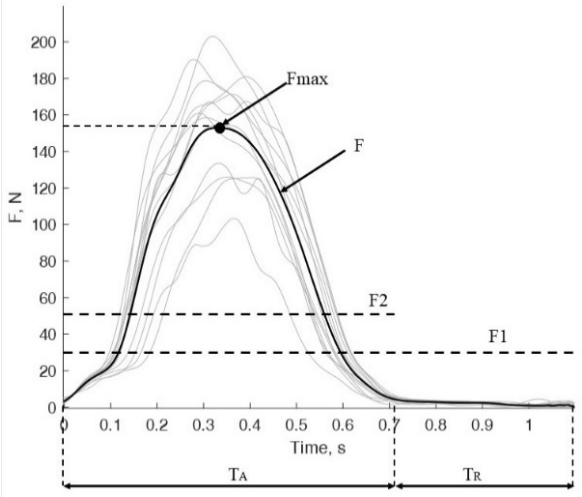

Fig. 7. Examples of overlap in the steady state phase of forces, F_i in grey and their mean F in black.

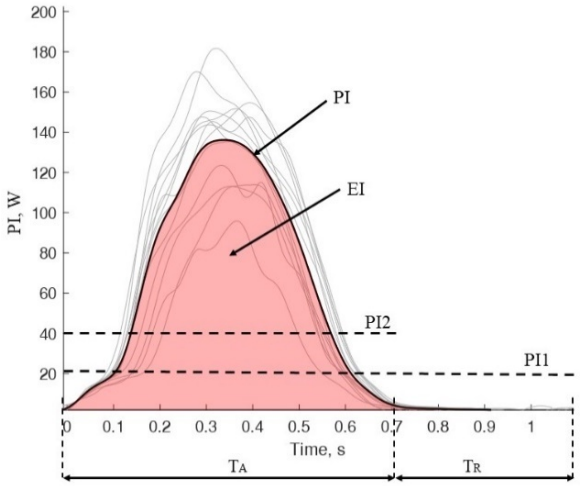

Fig. 8. Examples of overlap in the steady state phase of the input power, PI_i, in grey, and their mean *PI* in black, for a single run and the energy input *EI*, the red area.

wheelchair accelerates from zero to the steady-state speed. During the steady-state phase, the wheelchair speed oscillates around an average speed, as shown in Fig. 5. In Fig. 5 are also reported the right and left forces, in red and blue respectively. At the beginning of the acceleration phase, the wheelchair starts with a speed equal to zero. After five cycles, the steady-state speed is reached. At each cycle, the active time decreases because the wheelchair speed increases.

In Table 2, the means of the maximum forces, $F_{i,max}$ (SD), calculated over the five trials, are reported for each cycle, where the subscript i is the number of the cycle. In all the tests, the maximum force peak takes place in the second cycle. The force peaks are influenced by the characteristic "low" or "high" speed of the test and by the pulley radius, during the acceleration phase. For example, there is a slight difference by comparing test 1 and test 2 and a clear difference comparing test 1 and test 3.

During the steady-state phase, the wheelchair speed oscillates around the average value of the wheelchair steady-state speed $\bar{x}$ as it is shown in Fig. 5. In the steady-state phase, the active phase period T_A is almost constant for each test because the wheelchair speed oscillates around an average value. Figure 7 shows the overlap of the measured forces F_i of all the cycles of the

Table 3
Index *POF* (Peak of Force) calculated for three different kinds of propulsion. The index *POF* is the ratio between the mean of the useful force and the maximum force

System of propulsion	Test	$\dot{x}$ [m/s]	*POF*	*POF* [%]
Handwheelchair.Q	1	1.51	$POF = \frac{F2}{F_{max}}$	56
	2	1.63		54
	3	2.29		52
	4	2.36		45
Hand rim [25]	1	1.17	$POF = \frac{\text{mean}(F_{tan})}{\max(F_{res})}$	39
	2	1.37		44
	3	1.42		51
	4	1.64		47
	5	1.71		50
	6	2.52		38
	7	2.37		40
	8	2.37		41
	9	2.52		42
	10	2.45		45
Hand rim [26]	1	1.11	.	46
	2	1.66		41
	3	2.22		38
Handbike [21][a]	1		$POF = \frac{F_{tot\_trial}}{F_{peak}}$	56
	2			56
	3			61

[a][21] does not measure the longitudinal speed of the handbike.

steady-state phase, in grey, and their mean F, in black, for a single run. Also, $F1$, the average force during the complete cycle, $F2$, the average force during the active phase T_A, and F_{max}, the peak of F, are shown in Fig. 7. These values are listed for all tests in Table 2.

Figure 8 shows the overlap of the input powers PI_i of all the cycles of the steady state phase in grey and their mean *PI* in black, for a single run. Figure 8 also depicts *PI*1, the average power during the complete rowing gesture cycle, *PI*2, the average power during the active phase T_A, and the energy input *EI* as the red area under *PI*. These values for all tests are reported in Table 2.

In Table 2 the mean (*SD*) of some values of the steady state phase are reported. In the steady-state phase, the duration of the active phase, T_A, depends on the wheelchair speed and on the pulley radius. In fact, T_A decreases with increasing the wheelchair speed and with the increase of the pulley radius. On the other hand, the duration of the recovery phase, T_R, is almost constant. The mean of the input power over all complete cycles, *PI*1, increases when the wheelchair speed is increasing for all tests, as it should be. The average and the maximum forces depend on the wheelchair speed and on the pulley radius. In fact, in test 2 the forces are smaller than the ones of test 1 because $r_{p2} > r_{p1}$, even if the wheelchair speed of test 2 is higher than the one of test 1. The same reasoning is valid also for tests 3 and 4. Generally, the forces of tests 3 and 4 are higher than the forces of tests 1 and 2 due to the difference in wheelchair speed. A larger pulley enables the user to exert less force to achieve the same traction torque M_z. This is the reason why the forces in tests 2 and 4 are generally lower than the one in tests 1 and 3. Overall tests 3 and 4 requires more torque than tests 1 and 2 to move at a higher speed, thus the forces are higher during the faster tests. This pattern appears both during the acceleration phases and the steady-state phases. Obviously, during the acceleration phases, the peak force is larger than the steady state one because the wheelchair is accelerating.

The asymmetry of the right and left forces reported in Fig. 5, is due to the dominant side of the user, even if the trajectory of the test is straight. This asymmetry slightly affects the trajectory producing a minimal drift to one side, but, generally, the user keeps correcting unconsciously the trajectory by adjusting his/her force to maintain the trajectory straight. The same phenomenon appears also in conventional hand-rim wheelchairs because it is impossible to apply the exact same force to the two wheels. It is possible that part of the speed oscillations is due to the observed asymmetry. However, the main effect of this oscillation is the rowing gesture itself since it is made of two distinct phases. The figure clearly shows that during the active phase the measured speed increases whereas during the recovery phase it decreases.

Figure 9 is showing some details about the average acceleration phases of the four tests. The acceleration

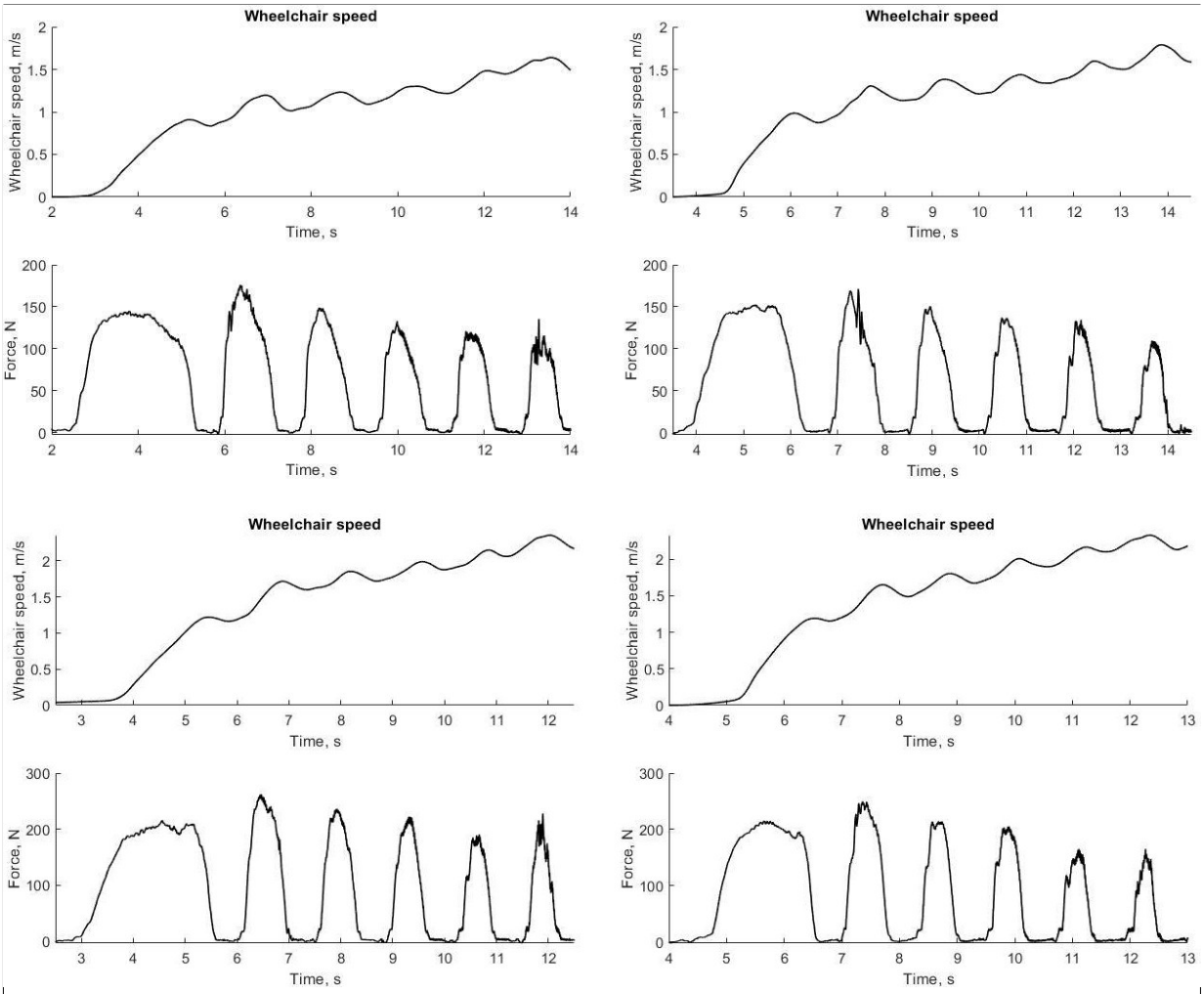

Fig. 9. Detail of average acceleration phases of the four tests.

phase duration is about the same for all tests regardless of the pulley radius. Because the user applies a lower force when a larger pulley is used and applies a larger force with a smaller pulley, the overall torque applied to the wheel is almost the same, therefore the acceleration times are similar. In case the same force was applied for both pulley radii, acceleration with the larger pulley would be faster.

4. Discussion

The indices *MEF* and *FEF* evaluate the efficiency of the wheelchair. For the standard wheelchair, these indices are lower than 100%, [21,25] due to the lateral and radial forces. For Handwheelchair.Q these indices are equal to 100% because the user force is entirely helpful for the transmission of motion under the hypothesis that the friction of the return pulley is negligible. In this prototype the return pulley is mounted on a couple of bearings, hence the actual value of the friction mainly depends on their quality. The index *POF* can be calculated for Handwheelchair.Q with the data of Table 2. In addition, the index *POF* can be calculated for a wheelchair with the hand rim system with the values reported in the paper [25], Table 3, and paper [26], Table 2, and for a handbike, [21], Table 3.1. Table 3 summarises the value of the index *POF* and Eq. (11) adjusted with the respective nomenclature. In any case, in the numerator, there is always the average useful force exerted by the user and in the denominator, there is the maximum force exerted. The mean value of *POF* for Handwheelchair.Q is 51.75%, while for the hand

rim wheelchair it is 43.7% in [25] and 41.6% in [26], and for the handbike in [21] it is 57.6%.

5. Conclusions

The aim of this paper was to analyse the propulsion force of a manual wheelchair with an innovative system of propulsion, Handwheelchair.Q. The force and the wheelchair speed were monitored during acceleration and steady-state phases of an experimental campaign. The paper shows that the forces depend on the wheelchair speed and on the pulley radius. The input power is obtained by the wheels' angular speed and the force. Future studies should focus on comparing the efficiency in the same test conditions of different manual wheelchair drive systems, such as handbikes, and hand-rims. For equal or similar wheelchair speeds, the larger pulley radius reduces the average and the maximum force, which are important to reduce the stress on the upper limb. The newly defined index *POF* has been calculated for Handwheelchair.Q, for two wheelchairs with the hand rim system and for a handbike. The index *POF* is lower for wheelchairs with the hand rim system than for Handwheelchair.Q, but it is higher for the handbike because in that system there is no recovery phase. A variable transmission ratio can be implemented on the proposed wheelchair in order to reduce the peak of force during the acceleration phase. F_{max} remains a fundamental parameter in order to evaluate the manual wheelchair, in addition, the direction of the force is relevant because it defines whether the shoulder and elbow joints are compressed or in traction. In future works, Handwheelchair.Q will be compared with hand rim wheelchairs, both from a mechanical and biomechanics point of view. In the next tests more subjects have to be included, wheelchair users in particular, in order to consolidate and validate the results obtained here. In addition, in the future it is important to compare the standard manual wheelchair and the Handwheelchair.Q in the same research setup.

Acknowledgments

The authors have no acknowledgments.

Author contribution

CONCEPTION: G. Quaglia and P. Cavallone.
PERFORMANCE OF WORK: A. Botta, P. Cavallone and L. Tagliavini.
INTERPRETATION OR ANALYSIS DATA: P. Cavallone.
PREPARATION OF THE MANUSCRIPT: A. Botta and P. Cavallone.
REVISION FOR INTELLECTUAL CONTENT: A. Botta, P. Cavallone, L. Tagliavini and G. Quaglia.
SUPERVISION: G. Quaglia.

Ethical considerations

The experimental protocol conformed with the Declaration of Helsinki and was approved by the Regional Ethics Committee (Commissione di Vigilanza, Servizio Sanitario Nazionale – Regione Piemonte – ASL 1 – Torino, Italy).

Conflict of interest

The authors have no conflicts of interest to report.

Funding

The authors report no funding.

References

[1] Lewis AR, Phillips EJ, Robertson WSP, Grimshaw PN, Portus M. Injury Prevention of Elite Wheelchair Racing Athletes Using Simulation Approaches. Proceedings. Multidisciplinary Digital Publishing Institute; 2018; 2: 255.
[2] Ballinger DA, Rintala DH, Hart KA. The relation of shoulder pain and range-of-motion problems to functional limitations, disability, and perceived health of men with spinal cord injury: a multifaceted longitudinal study. Arch Phys Med Rehabil. 2000; 81: 1575-81.
[3] Stirane D, Kiukucane E, Vetra A, Nulle A. The consequences of shoulder pain intensity on quality of life and community participation in paraplegic wheelchair users. SHS Web of Conferences. EDP Sciences; 2012; 2: 00033.
[4] Mashola MK, Korkie E, Mothabeng DJ. Pain and its impact on functioning and disability in manual wheelchair users with spinal cord injury: a protocol for a mixed-methods study. BMJ Open. British Medical Journal Publishing Group; 2021; 11: e044152.
[5] van Drongelen S, Arnet U, Veeger DHEJ, van der Woude LHV. Effect of workload setting on propulsion technique in handrim wheelchair propulsion. Med Eng Phys. 2013; 35: 283-8.
[6] van der Woude LHV, Formanoy M, de Groot S. Hand rim configuration: effects on physical strain and technique in unimpaired subjects? Med Eng Phys. 2003; 25: 765-74.
[7] Barbareschi G, Cheng T-J, Holloway C. Effect of technique and transfer board use on the performance of wheelchair transfers. Healthc Technol Lett. 2018; 5: 76-80.
[8] Barbareschi G, Sonenblum S, Holloway C, Sprigle S. Does the setting matter? Observing wheelchair transfers across different environmental conditions. Assist Technol. 2022; 34: 326-33.

[9] Arnet U, van Drongelen S, Scheel-Sailer A, van der Woude LHV, Veeger DHEJ. Shoulder load during synchronous handcycling and handrim wheelchair propulsion in persons with paraplegia. J Rehabil Med. 2012; 44: 222-8.

[10] Sasaki M, Stefanov D, Ota Y, Miura H, Nakayama A. Shoulder joint contact force during lever-propelled wheelchair propulsion. ROBOMECH Journal. 2015; 2: 13.

[11] Laschowski B, Mehrabi N, McPhee J. Optimization-based motor control of a Paralympic wheelchair athlete. Sports Eng. 2018; 21: 207-15.

[12] Haydon DS, Pinder RA, Grimshaw PN, Robertson WSP. Elite wheelchair rugby: a quantitative analysis of chair configuration in Australia. Sports Eng. 2016; 19: 177-84.

[13] Cooper RA, De Luigi AJ. Adaptive sports technology and biomechanics: wheelchairs. PM R. 2014; 6: S31-39.

[14] Sarraj AR, Massarelli R. Design History and Advantages of a New Lever-Propelled Wheelchair Prototype. International Journal of Advanced Robotic Systems. SAGE Publications; 2011; 8: 26.

[15] Quittmann OJ, Meskemper J, Abel T, Albracht K, Foitschik T, Rojas-Vega S, et al. Kinematics and kinetics of handcycling propulsion at increasing workloads in able-bodied subjects. Sports Eng. 2018; 21: 283-94.

[16] Cavallone P, Bonisoli E, Quaglia G. Prototyping of manual wheelchair with alternative propulsion system. Disabil Rehabil Assist Technol. 2020; 15: 945-51.

[17] Quaglia G, Bonisoli E, Cavallone P. The Design of a New Manual Wheelchair for Sport. Machines. 2019; 7: 31.

[18] Cavallone P, Bonisoli E, Quaglia G. Handwheelchair.q: New Prototype of Manual Wheelchair for Everyday Life. In: Niola V, Gasparetto A, editors. Advances in Italian Mechanism Science. Cham: Springer International Publishing; 2021. pp. 111-9.

[19] Quaglia G, Bonisoli E, Cavallone P. A proposal of alternative propulsion system for manual wheelchair. International Journal of Mechanics and Control. 2018; 19: 33-8.

[20] Bregman DJJ, van Drongelen S, Veeger HEJ. Is effective force application in handrim wheelchair propulsion also efficient? Clin Biomech (Bristol, Avon). 2009; 24:13-9.

[21] Arnet U, van Drongelen S, Veeger DH, van der Woude L HV. Force application during handcycling and handrim wheelchair propulsion: an initial comparison. J Appl Biomech. 2013; 29: 687-95.

[22] Moon Y, Jayaraman C, Hsu IMK, Rice IM, Hsiao-Wecksler ET, Sosnoff JJ. Variability of peak shoulder force during wheelchair propulsion in manual wheelchair users with and without shoulder pain. Clinical Biomechanics. 2013; 28: 967-72.

[23] Vanlandewijck Y, Theisen D, Daly D. Wheelchair propulsion biomechanics: implications for wheelchair sports. Sports Med. 2001; 31: 339-67.

[24] Veeger HEJ, van der Woude LHV, Rozendal RH. Load on the upper extremity in manual wheelchair propulsion. Journal of Electromyography and Kinesiology. 1991; 1: 270-80.

[25] Hernandez V, Gorce P, Rezzoug N. Evaluation and validation of musculoskeletal force feasible set indices: Application to manual wheelchair propulsion. J Biomech. 2018; 68: 70-7.

[26] Mason BS, Lenton JP, Goosey-Tolfrey VL. The physiological and biomechanical effects of forwards and reverse sports wheelchair propulsion. J Spinal Cord Med. 2015; 38: 476-84.